Inorg. Chem. **1989**, *28*, 3604–3606

Table III. Crystallographic Data for **2**

$TiO_3N_4C_{48}H_{64}$
fw: 792.97
$a = 24.597\ (4)$ Å
$b = 12.962\ (1)$ Å
$c = 29.373\ (4)$ Å
$\beta = 102.524\ (7)°$
$V = 9142\ (4)$ Å^3
$Z = 8$

space group: *C*20/*c* (no. 15)
$T = 21$ °C
$\lambda = 0.70930$ Å
$\rho_{calc} = 1.152$ g cm^{-3}
$\mu = 2.25$ cm^{-1}
$R(F_o) = 0.059$
$R_w(F_o) = 0.065$

cm^{-1} is shifted to 891 cm^{-1} when $^{18}OH_2$ was used in the synthesis of **2**. Much smaller shifts were observed (≤5 cm^{-1}) for the remaining bands, and hence we assign the band at 930 cm^{-1} as being due to the terminal titanium–oxo stretching frequency.

Experimental Section

Synthesis of Ti(O)(OAr-2,6Pr$^i_2$)$_2$(NC$_5$H$_4$-4NC$_4$H$_8$)$_2$ (2). To a solution of Ti(OAr-2,6Pr$^i_2$)$_2$[Bu^{t}NC(CH$_2$Ph)$_2$](py) (**1**) (0.50 g, 0.67 mmol) in benzene (25 mL) was added 4-pyrrolidinopyridine (0.30 g, 2.01 mmol). The mixture was stirred vigorously while water (12.1 μL, 0.67 mmol) was slowly added. After the mixture was stirred for 12 h, the benzene solvent was allowed to evaporate down slowly whereupon yellow crystals of the product began to form. The crystals were washed with hexane and dried under vacuum. Yield = 0.27 g (50%). Anal. Calcd for $TiC_{48}H_{64}N_4O_3$, (**2**)·C_6H_6: C, 72.71; H, 8.14; N, 7.07. Found: C, 71.85; H, 9.05; N, 7.29. ^{1}H NMR (C_6D_6, 30 °C): δ 3.23 (septet, C*H*Me$_2$), 1.29 (d, CH*Me*$_2$), 8.55 (d, ortho protons on pyridine ring), 6.11 (d, meta protons on pyridine ring), 2.68 (d), 1.36 (d, ortho and meta protons on pyrrolidine ring). Infrared (Nujol mull): ν(Ti–O), 930 cm^{-1}; ν(Ti–^{18}O), 891 cm^{-1}. Other IR bands (cm^{-1}): 3056 (w), 3022 (w), 2956 (s), 2924 (s), 2854 (s), 1612 (s), 1532 (s), 1484 (m), 1460 (s), 1434 (s), 1412 (s), 1378 (w), 1342 (w), 1330 (m), 1270 (s), 1224 (m), 1210 (m), 1180 (w), 1158 (w), 1110 (w), 1096 (w), 1066 (w), 1042 (w), 1014 (s), 930 (m), 894 (m), 874 (w), 816 (w), 804 (w), 748 (m), 706 (w), 682 (m), 660 (w).

Bu^{t}N(H)CH(CH$_2$Ph)$_2$. The organic amine was obtained from the hydrolysis supernatant by preparative TLC on silica eluted with a 1:1 benzene/hexane mixture. Yields typically were 70–85%. ^{1}H NMR (C_6D_6, 30 °C): δ 3.36 (broad, N*H*), 3.13 (quintet, C*H*(CH$_2$Ph)$_2$), 2.72 (AB pattern of doublets, CH(C*H*$_2$Ph)$_2$), 0.91 (s, C*Me*$_3$), 6.8–7.3 (aromatics). ^{13}C NMR (C_6D_6, 30 °C): 29.5 (C*Me*$_3$), 51.1 (*C*Me$_3$), 43.8 (*C*H$_2$Ph), 56.1 (C*H*), 126.3, 128.5, 130.0, 140.5 (CH$_2$*Ph*). High-resolution MS: calcd for $C_{19}H_{25}N$, 268.2065; found, 268.2061.

Crystallographic Studies

Selected crystal data and data collection parameters are collected together in Table III. A suitable crystal was mounted in a glass capillary in a random orientation. Cell constants and an orientation matrix for data collection were obtained from least-squares refinement by using the scattering angles of 25 reflections in the range 14.3° < θ < 17.2° as measured by the computer-controlled diagonal slit method of centering. Systematic absences and subsequent least squares refinement indicated the space group *C*2/*c* (no. 15). The data were collected at room temperature by using the ω–θ scan technique. The scan rate varied from 2 to 20°/min in ω, and data were collected to a maximum 2θ of 45°. Moving-crystal, moving-counter background counts were made by scanning an additional 25% above and below the scan width. The counter aperture was adjusted as a function of θ. For intense reflections an attenuator (factor 12.9) was automatically inserted in front of the detector. As a check on crystal and electronic stability, three standard reflections were remeasured every 5000 s of beam time. No decay in standards was observed.

The structure was solved by using the Patterson heavy-atom method to reveal the position of titanium atoms. The remaining heavy atoms were located in succeeding difference Fourier syntheses. Hydrogen atoms were located and added to the structures, but their positions were not refined. All calculations including the full-matrix least-squares refinement were performed by using Enraf-Nonius' SDP on a VAX computer.

Acknowledgment. We thank the National Science Foundation (Grant CHE-8612063) for support of this research.

Registry No. 1, 109284-20-0; **2**, 121919-40-2; *t*-BuNC(CH$_2$Ph)$_2$, 121935-24-8; *t*-BuN(H)CH(CH$_2$Ph)$_2$, 121935-25-9.

Supplementary Material Available: Listings of crystal data and data collection parameters, hydrogen atom parameters, anisotropic thermal parameters, and full bond distances and angles (14 pages); a listing of observed and calculated structure factors (19 pages). Ordering information is given on any current masthead page.

Contribution from the Department of Chemistry,
Washington State University,
Pullman, Washington 99164-4630

Temperature, Pressure, and Electrolyte Dependence of the Ferrocene/Ferrocenium Electron Self-Exchange in CD_3CN

Karl Kirchner, Shu-Qin Dang, Martin Stebler,
Harold W. Dodgen, Scot Wherland, and John P. Hunt*

Received May 1, 1989

We are studying the effects of elevated pressures on electron-transfer kinetics,[1,2] and the classic system ferrocene–ferrocenium is of interest. Wahl and co-workers[3] made an extensive study at atmospheric pressure via NMR spectroscopy some years ago. In the course of our research it appeared that our rate constants were somewhat larger than those reported by Wahl. Some results reported by Weaver et al.[4] also indicate a systematic difference with the earlier values. We have reinvestigated the system using 200-MHz NMR spectroscopy primarily in the hope of obtaining some more precise *k* values, which would be helpful in our elevated pressure work.

It is believed that $\Delta V^\ddagger$ measurements on a variety of electron-transfer reactions will aid in testing theories and providing more insight into detailed mechanisms. The ferrocene–ferrocenium case is attractive because formally 0/+1 interaction is involved and interpretation of the results may be facilitated in comparison to that of reactions involving more highly charged reactants. Unfortunately, there are experimental difficulties, particularly because of the fast exchange rate, which makes it hard to obtain extensive and/or precise $\Delta V^\ddagger$ values. We report here our best efforts in this case.

Experimental Section

Materials. Ferrocene (Fe(cp)$_2$) was purchased from Alfa Chemical Co. and was twice vacuum-sublimed. Fe(cp)$_2$PF$_6$ was prepared according to the literature.[3] Anal. Calcd: C, 36.29; H, 3.05; P, 9.35; F, 34.44. Found: C, 36.33; H, 2.97; P, 9.20; F, 32.33. The characteristic absorption band of ferrocenium was found at 617 ± 1 nm. The extinction coefficient was determined, from three independent experiments at 617 nm, to be 513.3 ± 9.5 M^{-1} cm^{-1} in acetonitrile under an argon atmosphere. Acetonitrile-d_3 was obtained from MSD Isotopes Merck, dried over 4-Å molecular sieves (activated at about 200 °C under vacuum), degassed by three freeze–pump–thaw cycles, and stored in an evacuated bulb in the dark until used. Co(cp)$_2$PF$_6$ was obtained from Strem Chemicals and used without further purification.

^{1}H NMR Measurements at 1 atm. Details of the sample preparations are given in ref 5. Proton NMR spectra were collected on a Nicolet NT200WB instrument. The aquisition parameters were a 4.5-μs pulse width, a 500-ms postaquisition delay, a 14 000-Hz sweep width, a 32K block size, and 500–4000 scans. Temperature readings were calibrated by using the method of Raiford et al.[6], corrected to 200 MHz, by adding a capillary of methanol to the experimental sample. The self-exchange rate was found to lie near the "fast-exchange" region. Therefore, the rate constants for electron exchange could be determined from eq 1,[3] where

$$k = \frac{4\pi x_D x_P (\delta\nu)^2}{(W_{DP} - x_P W_P - x_D W_D) C_{tot}} \qquad (1)$$

x_D and x_P are the mole fractions of diamagnetic and paramagnetic species, W_{DP}, W_P, and W_D are the NMR line widths (hertz) at half-height for the mixed, pure paramagnetic, and pure diamagnetic samples, respectively, $\delta\nu$ is the difference in resonance frequency (hertz) between

---

(1) (a) Nielson, R. M.; Hunt, J. P.; Dodgen, H. W.; Wherland, S. *Inorg. Chem.* **1986**, *25*, 1964. (b) Stebler, M.; Nielson, R. M.; Siems, W. F.; Hunt, J. P.; Dodgen, H. W.; Wherland, S. *Inorg. Chem.* **1988**, *27*, 2893.

(2) Kirchner, K.; Dodgen, H. W.; Wherland, S.; Hunt, J. P. *Inorg. Chem.* **1989**, *28*, 604.

(3) (a) Yang, E. S.; Chan, M.-S.; Wahl, A. C. *J. Phys. Chem.* **1980**, *84*, 3094. (b) Yang, E. S.; Chan, M.-S.; Wahl, A. C. *J. Phys. Chem.* **1975**, *79*, 2049.

(4) Nielson, R. M.; McManis, G. E.; Safford, L. K.; Weaver, M. J. *J. Phys. Chem.* **1989**, *93*, 2152.

(5) Anderson, K. A.; Wherland, S. *Inorg. Chem.* **1989**, *28*, 601.

(6) Raiford, D. S.; Fisk, C. L.; Becker, E. D. *Anal. Chem.* **1979**, *51*, 2050.

0020-1669/89/1328-3604$01.50/0

the pure paramagnetic and diamagnetic samples, and C_{tot} is the total molar concentration of the diamagnetic and paramagnetic species. Peak widths were determined by fitting the data to a Lorentzian line shape with use of the least-squares-minimizing program available on the Nicolet instrument. Typically, about 200 points above the base line were used in the fitting. The precise value for x_P was best determined from the chemical shift data by using eq 2,[4] where the subscripts are as before and

$$x_P = \frac{\nu_{DP} - \nu_D}{\delta\nu} \qquad (2)$$

ν is the resonance frequency. All chemical shifts are measured relative to tetramethylsilane (TMS). Errors in k were estimated from errors in parameters in eq 1.

The temperature-dependent data were fit to the Eyring equation. The errors in $\Delta H^{\ddagger}$ and $\Delta S^{\ddagger}$ are standard deviations calculated from the fitting program.

^1H NMR Measurements on Pressure Samples. The solutions were prepared in a dry nitrogen atmosphere in a glovebag or in the argon atmosphere of a drybox. The solutions were placed in a 4 mm o.d. × 3 cm glass NMR cell fitted with a sliding glass piston or a collapsible Teflon tube closed with a glass plug. The solutions were 35–70 mM in ferrocene and 4–7 mM in the ferrocenium hexafluorophosphate salt.

The proton NMR spectra were obtained at pressures from 0.1 to 200 MPa and temperatures from −8.5 to +10 °C on a Bruker WH-90 instrument fitted with a Be–Cu pressure bomb probe. Temperature was held constant (±0.1 °C) by circulating EtOH–H_2O from a thermostated bath through a jacket around the probe. The pressure was generated with a hand pump and read on an Astra gauge calibrated against a Heise gauge. The pressurizing fluid around the sample was 1,2-dibromotetrafluorethane (Gold Label, Aldrich Chemical Co.). TMS was used as an internal frequency standard and as a reference for field inhomogeneity determination (3–11 Hz).

NMR line widths and shifts were measured for ferrocene, ferrocenium, and mixtures thereof as a function of temperature and pressure. The spectra were transferred to a computer that displayed the experimental and digitally computed spectra simultaneously on an oscilloscope while adjusting parameters of the computed spectrum until a best visual fit was obtained. The shift and width of pure ferrocene were essentially independent of pressure and temperature. Pure ferrocenium shows a marked increase in line width with increasing pressure or decreasing temperature. The measured line widths are reproduced by eq 3, where W_P is the

$$\ln W_P = 3.7256 + 0.4064P/T + 852.3/T \qquad (3)$$

ferrocenium line width (fwhm) in Hz, P the pressure in MPa, and T the temperature in K. The maximum difference from the experimental widths is 4.7%, and the average is 1%. This equation implies a 3.4 cm^3 mol^{-1} volume of activation and a 1.7 kcal mol^{-1} energy of activation for the process controlling the ferrocenium line width. The shift between ferrocene and ferrocenium is given by eq 4, where $\delta\nu$ is in ppm. The shift is independent of pressure within 1%.

$$\delta\nu = 6790/(T - 50) \qquad (4)$$

The volume of activation, $\Delta V^{\ddagger} = -RT\,(\partial \ln k/\partial P)_T$, was found from a linear plot of ln k vs P, as shown in Figure 2. The slope is $-\Delta V^{\ddagger}/RT$.

Results

It is worth noting that the molar extinction coefficient of ferrocenium in acetonitrile as a solvent presented in this paper does not agree with values reported in the literature. In ref 3 an extinction coefficient of 446 M^{-1} cm^{-1} measured in the same solvent was found, and in ref 7 an extinction coefficient of 430 M^{-1} cm^{-1} measured in nitromethane was reported. Our value is 513 M^{-1} cm^{-1} for samples in an argon atmosphere, where decomposition should be minimal.

The chemical shift (ν_D) and the line width at half-height (W_D) of ferrocene are temperature independent. ν_D is 832.1 ± 0.5 Hz, and W_D is 0.7 ± 0.2 Hz. The chemical shifts and line widths of ferrocenium are strongly dependent on temperature. The data for the temperature dependence of shifts and line widths are fitted to a second-order polynomial function $y = a_0 + a_1x + a_2x^2$ ($a_0 = 6169.7 \pm 4.5$, $a_1 = -22.24 \pm 0.15$, $a_2 = 9.66 \times 10^{-2} \pm 7 \times 10^{-3}$ for the chemical shifts; $a_0 = 832.2 \pm 9.1$, $a_1 = -7.82 \pm 0.3$, $a_2 = 4.18 \times 10^{-2} \pm 0.01$ for the line widths). The values from the fitting function were used to obtain rate constants. Second-order rate constants k as a function of temperature and ferrocenium concentration are depicted in Figure 1. The activation parameters $\Delta H^{\ddagger}$ and $\Delta S^{\ddagger}$ are shown in Table II. Second-order rate constants measured at 25 °C in the presence of Co(cp)$_2$PF$_6$ and different Fe(cp)$_2$PF$_6$ concentrations are listed in Table I.

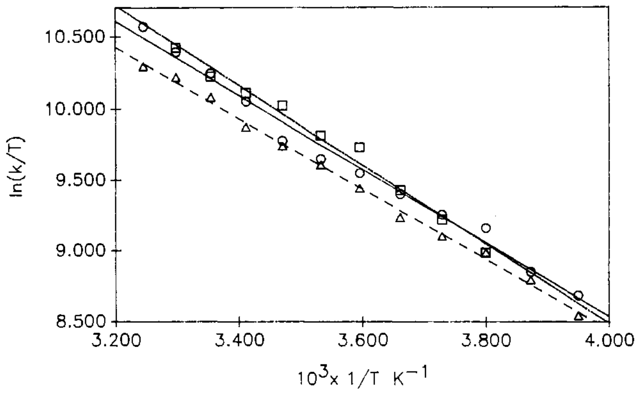

Figure 1. Eyring plots for electron-self-exchange rate constants of Fe(cp)$_2^{0/+}$ in CD$_3$CN: (○) [Fe(cp)$_2$] = 47.8 mM, [Fe(cp)$_2^+$] = 11.4 mM; (□) [Fe(cp)$_2$] = 45.2 mM, [Fe(cp)$_2^+$] = 17.8 mM; (△) [Fe(cp)$_2$] = 51.4 mM, [Fe(cp)$_2^+$] = 34.8 mM.

Table I. Second-Order Rate Constants at 25 ± 0.5 °C as a Function of Ferrocenium and Cobaltocenium

[Fe(cp)$_2$PF$_6$]/ mM	[Fe(cp)$_2$]/ mM	[Co(cp)$_2$PF$_6$]/ mM	$k \times 10^{-6}$/ M^{-1} s^{-1}
0.83[a]	18.1		9.3 ± 0.12
4.6[b]	24.7		8.6 ± 0.10
9.1	36.4		7.8 ± 0.06
11.4	47.8		8.2 ± 0.18
17.8	45.2		8.4 ± 0.07
1.6[c]	73.3	16.8	7.4 ± 2.0
34.8	51.4		7.1 ± 0.09
7.5[d]	45.2	33.3	6.9 ± 0.09

[a] $W_{DP} = 123.7 \pm 1.0$ Hz; $\nu_{DP} = 251.8 \pm 1.0$ Hz. [b] $W_{DP} = 315.7 \pm 2.0$ Hz; $\nu_{DP} = 883.2 \pm 1.7$ Hz. [c] $W_{DP} = 29.9 \pm 4.0$ Hz; $\nu_{DP} = 127.0 \pm 2.0$ Hz. [d] $W_{DP} = 229.7 \pm 1.8$ Hz; $\nu_{DP} = 814.2 \pm 1.9$ Hz.

Table II. Activation Enthalpies and Entropies of the Electron Self-Exchange between Fe(cp)$_2$ and Fe(cp)$_2$PF$_6$

[Fe(cp)$_2$PF$_6$]/mM	$\Delta H^{\ddagger}$/kcal mol^{-1}	$\Delta S^{\ddagger}$/cal mol^{-1} deg^{-1}
9.1	5.7 ± 0.3	−7.6 ± 1.0
11.4	5.3 ± 0.2	−9.0 ± 0.9
17.2	5.5 ± 0.3	−8.5 ± 1.0
34.8	4.9 ± 0.1	−10.7 ± 0.3

We have studied the pressure effects of k from −8.5 to −+10 °C and from 1 atm to 200 MPa. The system is near the "fast-exchange" regime, and it is difficult to obtain line broadenings that are primarily caused by the exchange process. Lowering temperature and total concentration helps, but one is limited by freezing of solvent and by solubility and signal/noise considerations. Two completely independent studies at −8.5 °C were made, and these have ca. 30–50% exchange broadening. We find $\Delta V^{\ddagger} = -4.5 \pm 1.0$ cm^3 mol^{-1} at −8.5 °C. At 0 °C we find $\Delta V^{\ddagger} = -8 \pm 1.8$ cm^3 mol^{-1}; at 5 °C $\Delta V^{\ddagger} = -7.9 \pm 0.8$ cm^3 mol^{-1}, and at 10 °C $\Delta V^{\ddagger} = -6.9 \pm 0.8$ cm^3 mol^{-1}. The average value for $\Delta V^{\ddagger}$ at the four temperatures is -7 ± 1 cm^3 mol^{-1}. The errors quoted are based on a least-squares fit, but we believe that an error of 2 cm^3 mol^{-1} is more realistic and that there is no evidence within the error for an effect of temperature on $\Delta V^{\ddagger}$. Much more accurate data would be required to test this conclusion. Some decomposition occurred in the pressure samples although they were prepared in an argon atmosphere. The decomposition products do not appear to affect k, and the mole fraction of Fe(III) was obtained from the shift measurements as was done by Wahl. A plot of ln k vs P at 0 °C is given in Figure 2.

Discussion

Ferrocenium ion decomposes in the presence of air and eventually gives a yellow-brown solid of unknown composition.

---

(7) Schmid, R.; Gutmann, V. *Monatsh. Chem.* **1973**, *104*, 864.

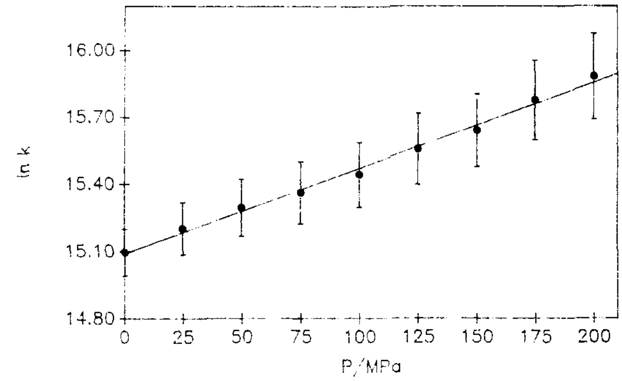

Figure 2. Activation volume data: natural logarithm of the rate constant vs pressure in MPa. $T = 0$ °C; $\{Fe(cp)_2\} = 37.2$ mM; $[Fe(cp)_2^+] = 2.7$ mM.

Samples for the atmospheric pressure studies were prepared on a vacuum line and showed no decomposition as noted by Wahl.[3]

The rate constants found in this work are larger than those of Wahl et al. by ca. 30–40%. Our k at 25 °C extrapolated to zero ionic strength is 9.3×10^6 M^{-1} s^{-1}, which can be compared with that of Weaver et al.[4] of 9.1×10^6 M^{-1} s^{-}–^{1} at $\mu = 0.65$ mM. The $\Delta H^{\ddagger}$ values we found agree quite well with those of Wahl (4.7 vs 5.3 kcal mol^{-1}), suggesting perhaps systematic errors in his rate constants. The rate constants are, in fact, very sensitive to the measured parameters. The errors are somewhat reduced at 200 MHz but are still of the order of ±5% at best.

There appears to be a small effect on k of changing the concentration of ferrocenium and/or addition of cobaltocenium. We find a decrease in k at 25 °C from $\mu = 0$ to μ 40 = mM of ca. 20%. The variation of ln k is fairly linear with $\mu^{1/2}$. One does not of course expect much effect on a 0/+1 reaction. The effect if any of μ on $\Delta H^{\ddagger}$ and $\Delta S^{\ddagger}$ is hard to assess. A similar effect, reduction of the rate constant with added salt, has been observed for the reduction of a series of cobalt(III) clathrochelates, +1 ions, by ferrocene[8] and for reactions between the neutral and +1 forms of the clathrochelates.[9] In these cases the effect has been attributed to a lower reactivity of ion-paired reactants.

A value for $\Delta V^{\ddagger}$ of -7.0 ± 2.0 cm^3 mol^{-1} is not significantly different from that found for the inner-sphere ruthenocene(II)–bromoruthenocene(IV) system (-3.0 ± 0.2 cm^3 mol^{-1}).[7] If the outer-sphere ferrocene–ferrocenium case involves some π–π^* ring interactions as suggested by Weaver et al.[10] and the ruthenium system involves a halo bridge, the factors influencing $\Delta V^{\ddagger}$ might be similar. Formation of a "bond" would lead to a negative $\Delta V^{\ddagger}$ contribution, release of solvent between the species gives a positive $\Delta V^{\ddagger}$ contribution, and diminished electrostriction effects in the activated complex would be small and lead to a positive contribution (we estimate ca. +1 cm^3 mol^{-1}).

In another approach, based on Marcus theory like model, the $\Delta V^{\ddagger}$ value is predicted from the solvent reorganization term,[11] eq 5, with an additional contribution from a precursor formation

$$\Delta V_{SR}^{\ddagger} = \frac{Ne^2}{16\epsilon_0\pi}\left[\frac{1}{r_{ab}} - \frac{1}{\sigma}\right]\left[\frac{\partial}{\partial P}\left[\frac{1}{n^2} - \frac{1}{\epsilon}\right]\right] \qquad (5)$$

constant. In eq 5, ϵ_0 is the permittivity of free space, r_{ab} is the assumed "radius" of the species, σ is the electron-transfer distance, n is the refractive index, and ϵ is the dielectric constant of the solvent. Assuming that r_{ab} and σ are pressure independent and using 4 Å for r_{ab} and 8 Å for σ,[12] this equation predicts a $\Delta V^{\ddagger}$ of ca. -15 cm^3 mol^{-1}. Larger values for r_{ab} and σ give more positive values for $\Delta V^{\ddagger}$. For example, an r_{ab} of 5 Å and a σ of 10 Å leads to a $\Delta V^{\ddagger}$ of ca. -12 cm^3 mol^{-1}. This is inconsistent with our result unless a large positive contribution to $\Delta V^{\ddagger}$ is made by precursor complex formation.

On the basis of a simple solvent electrostriction argument, a neutral and a +1 species should produce a transition state with a lower charge density and thus solvent should be released, leading to a positive $\Delta V^{\ddagger}$. Using a form of the Drude–Nernst equation presented previously,[1] we can roughly predict a value for $\Delta V^{\ddagger}$ of 1 cm^3 mol^{-1}. In the previous study[1] of electron self-exchange by manganese isocyanide complexes, both the simple Drude–Nernst equation and a method based on Marcus theory gave predictions that were not inconsistent with the results. However, in that case the reactants were +1 and +2 ions.

The lack of agreement with the above "theoretical" approaches emphasizes the need for a more detailed structural approach to $\Delta V^{\ddagger}$. Studies using a variety of solvents and substituted ferrocenes should be helpful in this regard. These studies should be done at higher magnetic fields when possible.

Acknowledgment. The authors wish to acknowledge the assistance of Don Appel with the NMR measurements. This work was supported by the National Science Foundation and by the Boeing Co. through funds for the purchase of the Nicolet instrument.

Registry No. Fe(cp)$_2$, 102-54-5; Fe(cp)$_2$PF$_6$, 11077-24-0; Co(cp)$_2$PF$_6$, 12427-42-8.

Supplementary Material Available: Tables of reactant concentrations, temperatures, rate constants, line widths, and chemical shifts (7 pages). Ordering information is given on any current masthead page.

---

[8] Borchardt, D.; Wherland, S. *Inorg. Chem.* **1984**, *23*, 2537.

[9] Gribble, J.; Wherland, S. *Inorg. Chem.*, in press.

[10] Nielson, R. M.; Golovin, M. N.; McManis, G. E.; Weaver, M. J. *J. Am. Chem. Soc.* **1988**, *110*, 1745.

[11] Swaddle, T. W. In *Inorganic High Pressure Chemistry*; van Eldik, R., Ed.; Elsevier: Amsterdam, 1986; Chapter 5.

[12] Dunitz, L. D.; Orgel, L. E.; Rich, A. *Acta Crystallogr.* **1956**, *9*, 373.

Contribution from the Department of Chemistry,
University of Wyoming, Laramie, Wyoming 82071

Synthesis and Characterization of a Bis(oxo)-Bridged Mn^{III}Mn^{III} Complex, Bis(μ-oxo)bis[N,N'-bis((6-methylpyrid-2-yl)methyl)ethane-1,2-diamine]dimanganese(III) Perchlorate

Patricia A. Goodson and Derek J. Hodgson*

Received March 21, 1989

Although manganese has long served as a practical oxidant for synthetic chemists, its role in several biological redox processes has only recently been the focus of study. In particular, a polynuclear manganese unit is now known to play an essential role in the oxidation of water to oxygen in photosystem II during photosynthesis.[1,2] Several research groups have focused their attention on the mixed-valent bis(μ-oxo)dimanganese(III/IV) system, [LMn(μ-O)$_2$MnL], a potential model for this biological redox process.[3] The first two complexes of this type, [(bpy)$_2$Mn^{III}(μ-O)$_2$Mn^{IV}(bpy)$_2$](ClO$_4$)$_3$ (bpy = 2,2'-bipyridine) and [(phen)$_2$Mn^{III}(μ-O)$_2$Mn^{IV}(phen)$_2$](ClO$_4$)$_3$ (phen = 1,10-phenanthroline), were synthesized in 1960.[4] No further examples of these compounds were generated until our report of [(bispicen)Mn^{III}(μ-O)$_2$Mn^{IV}(bispicen)](ClO$_4$)$_3$ (bispicen = N,N'-bis(2-pyridylmethyl)ethane-1,2-diamine) in 1987.[5] Since then, complexes have been reported with the tetradentate ligands tris(2-pyridylmethyl)amine,[6] tris(2-aminoethyl)amine,[7] 1,4,7,10-

---

[1] Beck, W. F.; Brudvig, G. W. *J. Am. Chem. Soc.* **1988**, *110*, 1517–1523 and references therein.

[2] Dismukes, G. C. *Photochem. Photobiol.* **1985**, *43*, 99–115.

[3] Matsushita, T.; Spencer, L.; Sawyer, D. T. *Inorg. Chem.* **1988**, *27*, 1167–1173.

[4] Nyholm, R. S.; Turco, A. *Chem. Ind. (London)* **1960**, 74–75.

[5] Collins, M. A.; Hodgson, D. J.; Michelsen, K.; Towle, D. K. *J. Chem. Soc., Chem. Commun.* **1987**, 1659–1660.

0020-1669/89/1328-3606$01.50/0